



Published in final edited form as:

Nat Cell Biol. 2013 January ; 15(1): 40–49. doi:10.1038/ncb2637.

Phosphorylation-enabled binding of Sgo1–PP2A to cohesin protects sororin and centromeric cohesion during mitosis

Hong Liu¹, Susannah Rankin², and Hongtao Yu^{1,*}

¹Department of Pharmacology, Howard Hughes Medical Institute, University of Texas Southwestern Medical Center, 6001 Forest Park Road, Dallas, TX 75390

²Program in Cell Cycle and Cancer Biology, Oklahoma Medical Research Foundation, Oklahoma City, OK 73104

Abstract

Timely dissolution of sister-chromatid cohesion in mitosis ensures accurate chromosome segregation to guard against aneuploidy and tumorigenesis. The complex of shugoshin and protein phosphatase 2A (Sgo1–PP2A) protects cohesin at centromeres from premature removal by mitotic kinases and Wapl in prophase. Here we address the regulation and mechanism of human Sgo1 in centromeric cohesion protection, and show that cyclin-dependent kinase (Cdk)-mediated, mitosis-specific phosphorylation of Sgo1 activates its cohesion-protection function and enables its direct binding to cohesin. The phospho-Sgo1-bound cohesin complex contains PP2A, Pds5, and hypophosphorylated sororin, but lacks Wapl. Expression of non-phosphorylatable sororin bypasses the requirement for Sgo1–PP2A in centromeric cohesion. Thus, mitotic phosphorylation of Sgo1 targets Sgo1–PP2A to cohesin, promotes dephosphorylation of Pds5-bound sororin, and protects centromeric cohesin from Wapl. PP2A-orchestrated, selective removal of a specific subset of phosphorylation from cohesin and its regulators underlies centromeric cohesion protection.

Timely establishment and dissolution of sister-chromatid cohesion during the cell cycle are critical for proper chromosome segregation and require cell-cycle-regulated modifications of cohesin and its regulators^{1–4}. Although the cohesin complex consisting of Smc1, Smc3, Scc1, and SA1/2 is already loaded onto chromatin in G1 phase, it remains dynamic. Concomitantly with DNA replication in S phase, a fraction of cohesin is converted to the cohesive state. This conversion requires Smc3 acetylation and, in human cells, subsequent binding of Pds5 and sororin to cohesin^{5–12}. Sororin competes with the cohesin inhibitor, Wapl, for Pds5 binding and opposes Wapl-mediated cohesin removal to establish cohesion in S phase¹¹.

Users may view, print, copy, download and text and data- mine the content in such documents, for the purposes of academic research, subject always to the full Conditions of use: http://www.nature.com/authors/editorial_policies/license.html#terms

*Correspondence: hongtao.yu@utsouthwestern.edu.

AUTHOR CONTRIBUTIONS

H.L. designed and performed all experiments and analyzed the data. H.Y. supervised the project and analyzed the data. S.R. provided key reagents and analyzed the data. H.L. and H.Y. wrote the paper.

COMPETING FINANCIAL INTERESTS

The authors declare that they have no competing financial interests.

Cohesion dissolution in mitosis occurs in two steps in human cells¹³. In prophase, the mitotic kinases Cdk1 and Plk1 phosphorylate sororin and SA2, respectively, to trigger Wapl-dependent removal of cohesin from chromosome arms^{11,14–17}. Phosphorylation of sororin disrupts the Pds5–sororin interaction, allowing Wapl to access Pds5 and remove cohesin from chromosome arms¹¹. The Sgo1–PP2A complex protects centromeric cohesin from the mitotic kinases and Wapl to enable bipolar attachment of sister chromatids to the mitotic spindle^{15,18–22}. After the satisfaction of the spindle checkpoint, the protease separase cleaves centromeric cohesin to allow sister-chromatid separation.

The mechanism by which human Sgo1–PP2A protects centromeric cohesion is not understood. How Sgo1 is regulated during the cell cycle is also unknown. Here we study the mechanism and regulation of Sgo1 in human cells. Our results establish a requirement for a phosphorylation–dephosphorylation cascade orchestrated by Cdk and Sgo1–PP2A in centromeric cohesion protection.

RESULTS

Cdk-dependent phosphorylation of human Sgo1 at T346 in early mitosis

Human Sgo1 underwent gel mobility shift in mitosis, consistent with it being phosphorylated¹⁹. To study whether Sgo1 phosphorylation was functionally important, we set out to systematically map the phosphorylation sites in Sgo1 in mitosis. We constructed doxycycline (Dox)-inducible HeLa cell lines that stably expressed siRNA-resistant Myc-Sgo1. Myc-Sgo1 was functional, as it rescued the premature sister-chromatid separation phenotype of Sgo1 RNAi cells^{18,23}. Furthermore, ectopic expression of Myc-Sgo1 did not alter cell cycle progression or the timing of chromosome segregation²³. Mass spectrometric analysis identified several phosphorylation sites in Myc-Sgo1 immunoprecipitated from mitotic cells (Fig. 1a and Supplementary Fig. 1a). We chose to focus on T346, which was conserved in vertebrate Sgo1 proteins (Fig. 1b). The T346A mutation abolished the slower-migrating Myc-Sgo1 bands on SDS-PAGE gels while the phosphorylation-mimicking T346D mutant had a slower mobility (Fig. 1c).

We next generated a phosphorylation-specific antibody against this site. This antibody only recognized the slower-migrating species of Myc-Sgo1 WT, but did not detect T346A, demonstrating its specificity (Fig. 1d). Furthermore, the phospho-T346-specific Sgo1 antibody detected the endogenous Sgo1 immunoprecipitated from nocodazole-arrested mitotic HeLa cells, but not that from thymidine-treated G1/S cells (Fig. 1e). Therefore, Sgo1 is phosphorylated at T346 specifically in mitosis.

Sgo1 localizes to centromeres in mitosis. We then examined the localization of phospho-T346 Sgo1. Our phospho-T346-specific Sgo1 antibody could not detect endogenous Sgo1 at centromeres. We thus stained HeLa cells stably expressing Myc-Sgo1 with this antibody. Phospho-T346 Sgo1 staining co-localized with that of Myc-Sgo1 at centromeres in prometaphase and metaphase, but disappeared in anaphase when Myc-Sgo1 signal was still present at centromeres (Fig. 1f). These results indicate that Sgo1 T346 phosphorylation occurs specifically during early mitosis.

The sequence flanking the Sgo1 T346 site is conserved and conforms to the Cdk phosphorylation consensus (Fig. 1b). Indeed, recombinant GST-Sgo1 was phosphorylated by cyclin B1/Cdk1 *in vitro*, as revealed by blotting with the phospho-T346-specific Sgo1 antibody (Fig. 1g). Furthermore, addition of the Cdk1 inhibitor, RO3306, to Taxol-arrested mitotic HeLa cells for 15 min greatly reduced T346 phosphorylation of both the endogenous Sgo1 and Myc-Sgo1 (Fig. 1h). By contrast, inhibition of Aurora B in the presence of Taxol and MG132 (which prevents mitotic exit) had a much less effect on T346 phosphorylation. Taken together, Sgo1 T346 can be phosphorylated by Cdk1 *in vitro*, and this phosphorylation is dependent on Cdk1 *in vivo*.

Sgo1 T346A is defective in centromeric cohesion protection

Sgo1 is phosphorylated at T346 in early mitosis when Sgo1 is expected to be active, and this phosphorylation is removed in anaphase. We tested whether Sgo1 T346 phosphorylation was indeed required for its function in centromeric cohesion. We constructed doxycycline (Dox)-inducible HeLa cell lines that stably expressed siRNA-resistant Myc-Sgo1 WT or T346A at similar levels (Supplementary Fig. 2a), and prepared mitotic chromosome spreads from these cells that had been depleted of the endogenous Sgo1 by RNAi (Fig. 2). Four major categories of mitotic chromosome morphology were observed (Fig. 2a). Most sister chromatids in categories I and II were unseparated while sister chromatids in categories III and IV were separated. As expected, depletion of Sgo1 caused massive premature sister-chromatid separation (Fig. 2b). Ectopically expressed Myc-Sgo1 WT largely rescued the cohesion defects of Sgo1 RNAi cells. By contrast, Myc-Sgo1 T346A was much less effective in the rescue, despite being expressed at a level comparable to that of Myc-Sgo1 WT (Fig. 2c). Similar results were obtained with different clones (Supplementary Fig. 2b). These results suggest that phosphorylation of Sgo1 at T346 is required for its function in centromeric cohesion.

We next sought to determine the mechanism by which T346 phosphorylation regulated Sgo1 in centromeric cohesion. Because both centromeric localization and PP2A binding were required for the function of Sgo1 in cohesion protection^{18,24}, we tested whether Sgo1 T346A was defective in either activity. Myc-Sgo1 T346A localized to mitotic centromeres with or without the endogenous Sgo1 depleted (Fig. 2d and Fig. 3a, b). Myc-Sgo1 T346A also bound to PP2A as efficiently as did Myc-Sgo1 WT (Fig. 3c). Thus, Sgo1 T346 phosphorylation is dispensable for centromeric localization and PP2A binding.

T346 phosphorylation enables Sgo1 binding to cohesin

Human Sgo1 has been shown to physically interact with cohesin²⁵. The functional relevance of this interaction is unclear, however. We tested whether Sgo1 phosphorylation regulated its binding to cohesin. We could not detect an interaction between the soluble cohesin and Myc-Sgo1 (Fig. 4a). However, upon nuclease-mediated digestion of chromosome DNA, we observed an association between Myc-Sgo1 and cohesin. Cohesin preferentially interacted with the slower-migrating, phospho-T346-containing Myc-Sgo1. Cohesin did not bind to Myc-Sgo1 T346A (Fig. 4a). We also observed an interaction between the endogenous cohesin and Sgo1 (Fig. 4b). This interaction was only present in mitosis, but not in G2.

Consistent with a requirement for Sgo1 phosphorylation in cohesin binding, cohesin only bound the slower-migrating, hyperphosphorylated Sgo1.

Our results indicate that phosphorylation of Sgo1 at T346 is required for Sgo1 binding to cohesin. Furthermore, the requirement of nuclease treatment to release the Sgo1–cohesin complex suggests that only the chromatin-associated cohesin binds to Sgo1, although this interaction does not require chromatin. Finally, the fact that mutation of a single residue in Sgo1 (T346A) disrupts both cohesin binding and cohesion protective function of Sgo1 strongly suggests that the Sgo1–cohesin interaction is functionally important.

The Sgo1–PP2A interaction is required for centromeric cohesion protection^{18,24}. We tested whether the Sgo1–cohesin complex also contained PP2A. Indeed, PP2A was present in both the cohesin complexes bound to Myc-Sgo1 or the endogenous Sgo1 (Fig. 4a, b). Like Sgo1, PP2A only interacted with cohesin in mitosis, not in G2. The mitosis-specific cohesin binding by PP2A depended on Sgo1, as depletion of endogenous Sgo1 abolished the interaction (Fig. 4b) and the cohesin-binding-deficient Myc-Sgo1 T346A failed to recruit PP2A to cohesin (Fig. 4a). Taken together, our results indicate that phospho-Sgo1 bridges the interaction between cohesin and PP2A.

We tested whether the phosphorylation-dependent Sgo1–cohesin interaction could be established *in vitro*, in the absence of chromatin and DNA replication. Recombinant GST-Sgo1 WT and T346A were incubated with or without Cdk1, bound to glutathione beads, and incubated with mitotic HeLa cell extracts. Phosphorylation of GST-Sgo1 WT by Cdk1 greatly stimulated T346 phosphorylation and Sgo1 binding to cohesin (Fig. 4c). GST-Sgo1 T346A did not bind to cohesin, with or without Cdk1, although it bound PP2A as efficiently as WT did. Conversely, affinity-purified cohesin from HeLa cells stably expressing Strep-SA2 with Strep-Tactin beads interacted with Cdk1-phosphorylated GST-Sgo1 WT, but not T346A (Fig. 4d). Thus, phosphorylation-dependent Sgo1 binding to cohesin can be established *in vitro*.

We further explored which cohesin subunit(s) mediated phospho-Sgo1 binding. Depletion of Scc1 or SA2 greatly reduced binding of Sgo1 to Smc1, while depletion of Wapl had no effect on Sgo1 binding (Fig. 4e). Moreover, Cdk1-phosphorylated GST-Sgo1 bound efficiently to the Scc1–SA2 complex expressed in Sf9 insect cells (Fig. 4f). These results implicate the Scc1–SA2 heterodimer as the binding partner of phospho-Sgo1, although the observed interaction might involve insect cell proteins.

Phospho-Sgo1–PP2A maintains cohesin-bound sororin in a hypophosphorylated state

Sgo1–PP2A had been proposed to protect SA2 from phosphorylation by Plk1, thereby maintaining centromeric cohesion^{21,26,27}. Surprisingly, we found that SA2 in the Sgo1–PP2A-bound cohesin remained phosphorylated at S1224, a known mitosis-specific Plk1 site¹⁴ (Fig. 5a, b). A large fraction of SA2 in Sgo1-bound cohesin still exhibited phosphorylation-dependent gel mobility shift (Fig. 5c). These data indicated that Sgo1–PP2A did not remove all phosphorylation from SA2. Indeed, no direct evidence supported SA2 dephosphorylation by Sgo1–PP2A in human cells. Furthermore, while it was clear that Sgo1–PP2A antagonized Wapl^{15,22}, it was unclear how SA2 dephosphorylation would

accomplish this task. On the other hand, a recent study established an antagonism between sororin and Wapl in cohesion establishment in S phase¹¹. Moreover, sororin underwent Cdk1-dependent phosphorylation and inactivation in mitosis^{11,16,17}. Finally and most importantly, a pool of sororin remained at the centromeres, and this localization required Sgo1 (Supplementary Fig. 3)¹¹. In contrast, depletion of sororin did not affect the centromeric localization of Sgo1 (Supplementary Fig. 3), despite the loss of cohesion. These results prompted us to test whether sororin was a downstream target of Sgo1–PP2A in centromeric cohesion protection in mitosis.

We first examined the binding of cohesion regulators to either total cohesin (which was immunoprecipitated by anti-Smc1) or phospho-Sgo1–PP2A-bound cohesin (which was immunoprecipitated by anti-Sgo1) during G2 and mitosis (Fig. 5d). In G2, Wapl, Pds5, and sororin all bound to total cohesin. In mitosis, sororin underwent hyperphosphorylation, as indicated by gel mobility shift retardation. While Wapl and Pds5A still bound to total cohesin in mitosis, binding of sororin to total cohesin was greatly reduced (Fig. 5d, e). By contrast, the phospho-Sgo1–PP2A-bound cohesin contained Pds5A and sororin, but lacked Wapl. Strikingly, the hypophosphorylated form of sororin preferentially interacted with Sgo1–PP2A-bound cohesin in mitosis (Fig. 5f). Similar to cohesin bound to endogenous Sgo1, cohesin bound to Myc-Sgo1 in mitosis also contained Pds5 and hypophosphorylated sororin, but lacked Wapl (Fig. 5g, h). These results suggested that Sgo1–PP2A might keep sororin in a hypophosphorylated state and maintain the Pds5–sororin interaction, thus antagonizing Wapl binding to cohesin.

We then tested whether sororin was a substrate of Sgo1–PP2A. We affinity-purified PP2A from HeLa cell extracts with recombinant GST-Sgo1 and incubated the partially purified GST-Sgo1–PP2A complex with Myc-sororin immunoprecipitated from mitotic cell extracts (Fig. 5i). Sgo1–PP2A diminished the hyperphosphorylated slower-migrating species of sororin, and addition of the PP2A inhibitor, okadaic acid, blocked this effect. Thus, sororin is indeed a substrate of Sgo1–PP2A.

Hypophosphorylated sororin antagonizes Wapl in mitosis

In mitosis, phospho-Sgo1–PP2A-bound cohesin contained Pds5 and hypophosphorylated sororin, but lacked Wapl. The centromeric localization of sororin in mitosis depended on Sgo1. These results suggested that Sgo1–PP2A at mitotic centromeres protected sororin, which antagonized Wapl as it did in interphase. We next sought to obtain more evidence for this hypothesis. We confirmed that co-depletion of Wapl rescued the mitotic arrest phenotype caused by Sgo1 depletion (Fig. 6a). Furthermore, similar to the depletion of Wapl¹⁵, overexpression of Sgo1 or sororin impeded the dissolution of chromosome arm cohesion in prophase and produced mitotic chromosomes with their arms closed (Fig. 6b, c). Consistent with T346 phosphorylation being critical for sister-chromatid cohesion, Sgo1 T346A was less efficient in inducing ectopic cohesion on chromosome arms. Depletion of sororin abolished the ectopic chromosome arm cohesion in prophase caused by Sgo1 overexpression (Fig. 6d). Sgo1 overexpression increased sororin binding and reduced Wapl binding to total cohesin (Fig. 6e). In contrast, sororin depletion allowed Wapl binding to Sgo1–PP2A-bound cohesin, without affecting Sgo1 or Pds5 binding (Fig. 6f). Taken

together, these results indicate that hypophosphorylated sororin in Sgo1–PP2A-bound cohesin antagonizes Wapl to protect centromeric cohesion.

Expression of non-phosphorylatable sororin bypasses the requirement for Sgo1–PP2A in centromeric cohesion

If the major function of Sgo1–PP2A is to dephosphorylate sororin and enable it to counteract Wapl, then ectopic expression of non-phosphorylatable sororin is expected to bypass the requirement for Sgo1–PP2A in sister-chromatid cohesion. Recent studies showed that mutation of all 9 potential Cdk sites in sororin to alanine (9A) eliminated hyperphosphorylated slower-migrating species of sororin in mitosis and delayed sororin and cohesin release from chromosome arms¹⁶. We tested whether expression of sororin-GFP 9A could bypass the requirement for Sgo1 or PP2A in centromeric cohesion. We constructed doxycycline-inducible HeLa cell lines that expressed sororin-GFP WT or 9A at levels comparable to that of the endogenous sororin (Fig. 7a and Supplementary Fig. 4a). Expression of either sororin-GFP WT or 9A substantially rescued the mitotic arrest phenotype of sororin depletion (Supplementary Fig. 4b), indicating that both GFP fusion proteins were functional and that phosphorylation of sororin at these sites was not required for its mitotic function. Strikingly, while expression of sororin-GFP WT only marginally rescued the cohesion defects caused by Sgo1 or PP2A depletion, expression of sororin-GFP 9A largely eliminated such defects (Fig. 7b, c).

Both Sororin-GFP WT and 9A were concentrated at centromeres, although 9A had stronger signals on chromosome arms (Fig. 7d). Consistent with the inability of sororin WT to bypass the requirement for Sgo1 in centromeric cohesion, depletion of Sgo1 abolished the centromeric localization of sororin-GFP WT (Fig. 7d). On the other hand, depletion of Sgo1 did not appreciably alter the centromere localization of sororin-GFP 9A (Fig. 7d), explaining why sororin 9A was able to bypass the requirement for Sgo1 in cohesion protection.

To further test the involvement of Cdk1 in regulating sororin, we treated mitotic control, siSgo1, or siPP2A cells with the Cdk1 inhibitor RO3306 for 15 minutes and then examined the sororin-GFP localization in these cells. In control and siSgo1 cells treated with RO3306, chromosomes became decondensed, and sororin-GFP associated with the decondensed chromatin, including centromeres (Supplementary Fig. 5). Although this result was consistent with the Cdk1 activity preventing sororin association with chromosomes, chromosome binding of sororin-GFP in RO3306-treated cells could be an indirect consequence of chromosome decondensation or mitotic exit. On the other hand, about 55% of the siPP2A cells treated with RO3306 remained in mitosis and contained condensed chromosomes (Fig. 8a), perhaps because of a role of PP2A in mitotic exit²⁸. Strikingly, sororin-GFP was detected at the centromeres and other chromosome regions in these cells. This result strongly suggests that the dissociation of sororin-GFP from centromeres in siPP2A cells is dependent on the Cdk1 activity.

DISCUSSION

Chromosome missegregation in mitosis leads to aneuploidy, which can drive tumorigenesis under certain contexts. Indeed, mutations of cohesin and its regulators have been linked to

human diseases, including cancer^{2,29}. A better understanding of cohesion establishment and maintenance will help to decipher the underlying causes of these human diseases and identify new molecular targets for drug intervention. Our study provides key insights into both regulation and mechanism of the critical centromeric cohesion protector Sgo1. Our results support a model in which Sgo1 is activated by Cdk-dependent phosphorylation at T346 during early mitosis in human cells (Fig. 8b). Phospho-Sgo1 binds directly to cohesin and bridges an interaction between cohesin and PP2A. The cohesin-bound PP2A keeps sororin in a hypophosphorylated state and maintains the Pds5–sororin interaction to counteract Wapl.

In fission yeast, fusing a PP2A subunit to a cohesin subunit artificially recruited PP2A to chromosomes and blocked cohesin removal and chromosome segregation in meiosis in a Sgo1-independent manner²⁷. This result led to the proposal that the sole function of Sgo1 in cohesion protection was to recruit PP2A to centromeres. The situation appears to be more complex in mammals. There are two shugoshin proteins, Sgo1 and Sgo2, in mammals²¹. Depletion of Sgo1 in human cells causes massive chromosome missegregation, but does not appreciably alter the centromeric localization of PP2A^{18,21}. By contrast, Sgo2 is required for PP2A centromeric targeting in human cells²¹, but is largely dispensable for chromosome segregation during mitosis³⁰. In fact, Sgo2 knockout mice are viable but infertile³¹, indicating that mammalian Sgo2 is specifically required for meiosis, but not for mitosis. Therefore, the centromeric targeting of PP2A is neither necessary nor sufficient for cohesion protection during mitosis in human cells.

The current study reconciles these disparate findings. Our results indicate that Sgo1 has two separable functions in mitosis: (1) targeting a pool of PP2A to centromeres, and (2) recruiting PP2A to cohesin through directing binding to cohesin. The second function of Sgo1 is only activated during early mitosis through Cdk1-dependent phosphorylation. The phospho-deficient Sgo1 T346A mutant binds to PP2A and localizes normally to centromeres, but it fails to support proper chromosome segregation during mitosis. Thus, in addition to the centromeric recruitment of PP2A, cell-cycle-regulated, direct binding of cohesin by Sgo1 is an indispensable function of Sgo1 in centromeric cohesion protection. Fusion of PP2A to a cohesin subunit in yeast induces Sgo1-independent cohesion protection in meiosis, presumably because this fusion protein bypasses both the PP2A-targeting and cohesin-binding functions of Sgo1. In mammalian somatic cells, a large fraction of centromeric PP2A is bound and recruited to centromeres by Sgo2, which does not bind to mitotic forms of cohesin²⁵. Sgo2 and the centromeric pool of PP2A bound to it are both dispensable for centromeric cohesion protection during the mitotic cell cycle.

The enrichment of endogenous Sgo1 at centromeres requires Bub1-mediated phosphorylation of H2A^{32,33}, suggesting that the Bub1-H2A axis is required for restricting the phospho-Sgo1-PP2A-cohesin complex to centromeres. On the other hand, overexpression of Sgo1 generates ectopic cohesion along chromosome arms, in a mechanism requiring Sgo1 T346 phosphorylation. Thus, the phospho-Sgo1-PP2A-cohesin complex can form at non-centromere chromosome regions.

What then are the relevant substrates of cohesin-bound Sgo1–PP2A at centromeres in human cells? One substrate of PP2A appears to be Sgo1 itself¹⁸. Depletion of PP2A abolishes Sgo1 binding to centromeres, which is restored by Plk1 co-depletion¹⁸. PP2A directly reverses Plk1-mediated phosphorylation of Sgo1 *in vitro*, and depletion of PP2A greatly reduces cohesin binding by Myc-Sgo1 in HeLa cells (data not shown). These findings suggest that PP2A protects Sgo1 from Plk1-dependent removal from chromatin and cohesin. Previous studies have also implicated SA2 phosphorylated by Plk1 as a substrate of Sgo1–PP2A in centromeric cohesion protection^{21,26,27}. PP2A does not, however, remove all phosphorylation of SA2 in the Sgo1–PP2A-bound pool of cohesin. Furthermore, expression of non-phosphorylatable SA2 only partially alleviates the cohesion defect caused by Sgo1 depletion²⁶, indicating the existence of additional PP2A substrates in this process. We show here that Sgo1–PP2A-bound cohesin contains Pds5 and hypophosphorylated sororin, but lacks Wapl. Ectopic expression of a non-phosphorylatable mutant of sororin largely bypasses the requirement for Sgo1–PP2A in cohesion protection. Together with the previous finding that depletion of Sgo1 abolishes the centromeric targeting of sororin¹¹ (which we confirm in our study), our results establish sororin as a critical downstream target of Sgo1–PP2A in centromeric cohesion protection. Sgo1 does not directly recruit sororin, but maintains sororin binding to Pds5 and cohesin through PP2A-dependent dephosphorylation. Hypophosphorylated sororin competes with the well-established cohesion inhibitor Wapl for binding to Pds5 and cohesin in mitosis, readily explaining how sororin dephosphorylation by Sgo1–PP2A protects cohesion.

The spatiotemporally confined, dynamic tug of war between mitotic kinases and PP2A thus underlies centromeric cohesion protection in mitosis (Fig. 8b). In this process, Cdk1-dependent phosphorylation of two positive cohesin regulators in the same complex has opposing functions. Phosphorylation of sororin inhibits cohesion. Phosphorylation of Sgo1 by Cdk1 promotes PP2A-mediated dephosphorylation of sororin, thereby maintaining cohesion. How PP2A selectively dephosphorylates sororin without affecting Sgo1 phosphorylation at specific sites remains to be determined. Nevertheless, our study provides an astounding example that epitomizes the importance of spatiotemporally regulated, reversible posttranslational modifications of proteins in fast biological processes, including chromosome segregation and mitotic progression.

METHODS

Mammalian cell culture and transfection

HeLa Tet-On (Invitrogen) cells were grown in Dulbecco's modified Eagle's medium (DMEM; Invitrogen) supplemented with 10% fetal bovine serum and 10 mM L-glutamine. To arrest cells at G1/S, cells were incubated in the growth medium containing 2 mM thymidine (Sigma) for 17 hr. G2 cells were collected at 7 hr after the release from thymidine arrest. Mitotic cells were obtained by adding 300 nM nocodazole (Sigma) at 8 hr after the release from thymidine arrest and incubating for another 4 hr.

Plasmid transfection was performed when cells reached a confluency of about 40–60% using the Effectene reagent (Qiagen) per manufacturer's protocols. To establish stable cell lines, HeLa Tet-On cells were transfected with pTRE2 vectors encoding RNAi-resistant

Myc-Sgo1 WT, Myc-Sgo1 T346A, sororin-GFP WT, and sororin-GFP 9A and selected with 300 µg/ml hygromycin (Invitrogen). The surviving clones were screened for expression of the desired proteins in the presence of 1 µg/ml doxycycline (Invitrogen). To obtain HeLa Tet-On cell lines that constitutively express RNAi-sensitive sororin-GFP WT, cells were transfected with pIRES-sororin-GFP and selected with 500 ng/ml puromycin (Sigma).

For RNAi experiments, the siRNA oligonucleotides were purchased from Thermo Scientific. HeLa cells were transfected using Lipofectamine RNAiMax (Invitrogen) and analyzed at 24–48 hr after transfection. The sequences of the siRNAs used in this study are: Sgo1 siRNA (GAGGGGACCCUUUACAGATT), PP2A siRNA1 (GGACCCGAAGUGAGCUUCUTT), sororin siRNA (siGENOME MQ-015256-01-0002, Thermo Scientific), Pds5A siRNA (MQ-014071-02-0002, Thermo Scientific), Pds5B siRNA (MQ-010362, Thermo Scientific), Wapl siRNA (CGGACTACCCTTAGCACAA), Scc1 (MQ-006832-01-002, Thermo Scientific), and SA2 (MQ-021351-01-0002, Thermo Scientific).

Antibodies, immunoblotting, and immunoprecipitation

The α -Sgo1-pT346 antibody was produced in an in-house facility by immunizing rabbits with the synthetic peptide (GVHLPTPFRQC) coupled to hemocyanin (Sigma). The production of the anti-sororin and anti-Wapl antibodies was described previously^{34,35}. The following antibodies were purchased from the indicated sources: CREST (ImmunoVision, HCT-0100), α -Myc (Roche, 11667203001), α -PP2A A α (Santa Cruz, sc-6112), α -SA2 (Bethyl, A300-158A), α -Pds5A (Bethyl, A300-088A), α -Pds5B (Bethyl, A300-537A), α -Smc1 (Bethyl, A300-055A), α -Smc3 (Bethyl, A300-060A), α -Scc1 (Bethyl, A300-080A), Wapl (Bethyl, A300-268A), α -H3pS10 (Millipore, 05-1336), α -MPM2 (Millipore, 05-368) and α -GFP (Aves Labs, GFP-1020).

For immunoblotting, the antibodies were used at 1:1000 dilution for crude sera or at 1 µg/ml for purified and monoclonal antibodies. For immunoprecipitation, α -Smc1, α -Myc, or affinity-purified α -Sgo1 antibodies were coupled to Affi-Prep Protein A beads (Bio-Rad) at a concentration of 1 mg/ml. HeLa cells were lysed with the Lysis Buffer [25 mM Tris-HCl pH 7.5, 75 mM NaCl, 5 mM MgCl₂, 0.1% NP-40, 1 mM DTT, 0.5 µM okadaic acid, 5 mM NaF, 0.3 mM Na₃VO₄, 10 mM β -glycerophosphate, and 50 units/ml Turbo-nuclease (Accelagen)]. After a 2-hr incubation on ice and then a 10-min incubation at 37°C, the lysate was cleared by centrifugation for 20 min at 4°C at 14,000 rpm. The supernatant was incubated with the antibody beads for 2 hr at 4°C. The beads were washed four times with the Lysis Buffer. The proteins bound to the beads were dissolved in SDS sample buffer, separated by SDS-PAGE, and blotted with the appropriate antibodies. The Myc immunoprecipitates from 16 dishes (150 mm) of HeLa Tet-On cells stably expressing Myc-Sgo1 were resolved on SDS-PAGE and stained with GelCode Blue (Thermo Scientific). Protein bands were excised from the gel, digested with trypsin and AspN, and analyzed by mass spectrometry to map phosphorylation sites.

Immunofluorescence and chromosome spread

Mitotic cells collected by shake-off were washed once with PBS and spun onto microscope slides with a Shandon Cytospin centrifuge. Cells were first extracted with PBS containing 0.3% Triton X-100 for 5 min and then fixed in 4% paraformaldehyde for 15 min. After washing three times with PBS containing 0.1% Triton X-100, the cells were incubated with the appropriate primary antibodies and CREST in PBS containing 3% BSA and 0.1% Triton X-100. The cells were washed three times with PBS containing 0.1% Triton X-100 for 5 min each time and incubated with fluorescent secondary antibodies (Molecular Probes) in PBS containing 0.1% Triton X-100 and 3% BSA for 1 hr. The cells were again washed three times with PBS containing 0.1% Triton X-100 and stained with 1 $\mu\text{g/ml}$ DAPI for 1 min. After the final washes, the slides were sealed and viewed using a 63X objective on a Deltavision microscope (Applied Precision). A series of z-stack images was captured at 0.4- μm intervals, deconvolved, and projected. Image processing and quantification were done with ImageJ. For Myc-Sgo1 staining, a mask was generated to mark all centromeres based on CREST staining in the projected image. After background subtraction, the mean intensity for objects in the mask in each channel was measured. These values were then normalized by the intensity of CREST signals, and plotted with the Prism software. For pT346 Sgo1 staining, the mean intensity was normalized to Myc-Sgo1. For each condition, centromeric staining of at least 18 mitotic cells was measured.

For chromosome spreads, mitotic cells were swelled in H_2O , and fixed with methanol:acetic acid (v/v = 3:1) for 15 min at room temperature. Cells were dropped onto microscope slides, dried at room temperature, and stained with Giemsa (EMD). The slides were washed, sealed, and analyzed as described above. For centromeric staining of chromosome spreads, mitotic cells were swelled in a pre-warmed hypotonic solution containing 55 mM KCl for 15 min at 37°C and spun onto slides. Chromosomes were fixed and stained as described for whole-cell staining.

Kinase assays, protein-binding assays, and phosphatase assays

Recombinant GST-Sgo1 WT and T346A and cyclin B1-Cdk1 were expressed in Sf9 cells and purified as previously described¹⁹. GST-Sgo1 WT and T346A were incubated cyclin B1-Cdk1 in the kinase buffer (50 mM Tris-HCl pH 7.5, 300 mM NaCl, 5 mM MgCl_2 , 0.1% NP-40, 1 mM DTT, 0.5 μM Okadaic Acid, 5 mM NaF, 0.3 mM Na_3VO_4 , 10 mM β -glycerophosphate, and 100 μM ATP) at room temperature for 1hr. The reaction was quenched by the addition of sample buffer. Samples were resolved on SDS-PAGE followed by Coomassie blue staining or immunoblotting with α -pT346 Sgo1.

For GST pull-down assays, recombinant GST-Sgo1 WT and TA phosphorylated by cyclin B1-Cdk1 as described above were immobilized on glutathione-Sepharose beads (GE Healthcare) and incubated with lysates of mitotic HeLa cells or Sf9 cells expressing Scc1-His₆ and SA2 at 4°C for 1 hr. The beads were washed four times with the Lysis Buffer. The proteins bound to beads were dissolved in sample buffer, resolved on SDS-PAGE, and blotted with antibodies against GST, pT346 Sgo1, cohesin, and PP2A.

For Strep pull-down assays, the mitotic cells stably expressing StrepII-SA2 were lysed with the Lysis Buffer containing 250 mM (total) NaCl. The lysate was incubated with Strep-Tactin beads (Qiagen) at 4°C for 1 hr. The beads were washed twice with the Lysis Buffer containing 250 mM NaCl, twice with the Lysis Buffer containing 450 mM NaCl, and incubated at 4°C for 1 hr with GST-Sgo1 WT and T346A pre-treated with cyclin B1-Cdk1. The beads were washed four times with the Lysis Buffer containing 50 mM NaCl. The proteins bound to beads were dissolved in sample buffer, resolved on SDS-PAGE, and blotted with antibodies against Sgo1, pT346 Sgo1, and SA2.

For the phosphatase assay, GST-Sgo1 was incubated with mitotic HeLa cell extracts in the Lysis Buffer containing 250 mM NaCl at 4°C for 1 hr. Glutathione-Sepharose beads were then added to pull down GST-Sgo1-PP2A. After washing four times with the Lysis Buffer containing 250 mM NaCl, the proteins bound to beads were eluted with the Lysis Buffer containing 250 mM NaCl and 10 mM reduced L-glutathione. Hyperphosphorylated Myc-sororin was immunoprecipitated with α -Myc beads from lysates of mitotic HeLa cells transfected with a Myc-sororin plasmid. The Myc-sororin beads were then incubated with GST-Sgo1-PP2A with or without 1 mM okadaic acid in the phosphatase buffer (25 mM Tris-HCl pH 7.5, 250 mM NaCl, 5 mM MgCl₂, 0.1% NP-40, and 1 mM DTT) at 30°C for 1 hr. Samples were resolved on SDS-PAGE and blotted with antibodies against GST, PP2A, and sororin.

Flow cytometry

Cells were collected with trypsinization and fixed with ice-cold 70% ethanol overnight. After washing with PBS, the fixed cells were permeabilized with 0.25% Triton X-100 on ice for 5 min and incubated with α -MPM2 at room temperature for 3 hr. After washing with PBS containing 1% BSA, the cells were resuspended with the secondary antibody and incubated for 1 hr. After washing with PBS, the cells were resuspended in PBS containing RNase A and propidium iodide, and analyzed with a flow cytometer. Results were processed with FlowJo.

Supplementary Material

Refer to Web version on PubMed Central for supplementary material.

ACKNOWLEDGEMENTS

We thank Yan Li and the Protein Chemistry Core at UT Southwestern Medical Center for mass spectrometry analysis of phospho-Sgo1. We also thank Jingrong Chen for making the sororin antibody and Jan-Michael Peters for providing the phospho-S1224-SA2 antibody. S.R. was funded by grant RR016478 from the National Center for Research Resources (NCRR), a component of the National Institutes of Health (NIH), and is a Pew Scholar in the Biomedical Sciences. H.Y. is an Investigator with the Howard Hughes Medical Institute and is supported by grants from the Welch Foundation (I-1441), and the Cancer Prevention Research Institute of Texas (RP110465).

REFERENCES

1. Nasmyth K. Cohesin: a catenase with separate entry and exit gates? *Nat. Cell Biol.* 2011; 13:1170–1177. [PubMed: 21968990]
2. Peters JM, Tedeschi A, Schmitz J. The cohesin complex and its roles in chromosome biology. *Genes Dev.* 2008; 22:3089–3114. [PubMed: 19056890]

3. Onn I, Heidinger-Pauli JM, Guacci V, Unal E, Koshland DE. Sister chromatid cohesion: a simple concept with a complex reality. *Annu. Rev. Cell Dev. Biol.* 2008; 24:105–129. [PubMed: 18616427]
4. Sherwood R, Takahashi TS, Jallepalli PV. Sister acts: coordinating DNA replication and cohesion establishment. *Genes Dev.* 2010; 24:2723–2731. [PubMed: 21159813]
5. Rankin S, Ayad NG, Kirschner MW. Sororin, a substrate of the anaphase-promoting complex, is required for sister chromatid cohesion in vertebrates. *Mol. Cell.* 2005; 18:185–200. [PubMed: 15837422]
6. Schmitz J, Watrin E, Lenart P, Mechtler K, Peters JM. Sororin is required for stable binding of cohesin to chromatin and for sister chromatid cohesion in interphase. *Curr. Biol.* 2007; 17:630–636. [PubMed: 17349791]
7. Rolef Ben-Shahar T, et al. Eco1-dependent cohesin acetylation during establishment of sister chromatid cohesion. *Science.* 2008; 321:563–566. [PubMed: 18653893]
8. Unal E, et al. A molecular determinant for the establishment of sister chromatid cohesion. *Science.* 2008; 321:566–569. [PubMed: 18653894]
9. Rowland BD, et al. Building sister chromatid cohesion: smc3 acetylation counteracts an antiestablishment activity. *Mol. Cell.* 2009; 33:763–774. [PubMed: 19328069]
10. Zhang J, et al. Acetylation of Smc3 by Eco1 is required for S phase sister chromatid cohesion in both human and yeast. *Mol. Cell.* 2008; 31:143–151. [PubMed: 18614053]
11. Nishiyama T, et al. Sororin mediates sister chromatid cohesion by antagonizing Wapl. *Cell.* 2010; 143:737–749. [PubMed: 21111234]
12. Lafont AL, Song J, Rankin S. Sororin cooperates with the acetyltransferase Eco2 to ensure DNA replication-dependent sister chromatid cohesion. *Proc. Natl. Acad. Sci. U. S. A.* 2010; 107:20364–20369. [PubMed: 21059905]
13. Waizenegger IC, Hauf S, Meinke A, Peters JM. Two distinct pathways remove mammalian cohesin from chromosome arms in prophase and from centromeres in anaphase. *Cell.* 2000; 103:399–410. [PubMed: 11081627]
14. Hauf S, et al. Dissociation of cohesin from chromosome arms and loss of arm cohesion during early mitosis depends on phosphorylation of SA2. *PLoS Biol.* 2005; 3:e69. [PubMed: 15737063]
15. Kueng S, et al. Wapl controls the dynamic association of cohesin with chromatin. *Cell.* 2006; 127:955–967. [PubMed: 17113138]
16. Dreier MR, Bekier ME 2nd, Taylor WR. Regulation of sororin by Cdk1-mediated phosphorylation. *J. Cell Sci.* 2011; 124:2976–2987. [PubMed: 21878504]
17. Zhang N, Panigrahi AK, Mao Q, Pati D. Interaction of Sororin Protein with Polo-like Kinase 1 Mediates Resolution of Chromosomal Arm Cohesion. *J. Biol. Chem.* 2011; 286:41826–41837. [PubMed: 21987589]
18. Tang Z, et al. PP2A is required for centromeric localization of Sgo1 and proper chromosome segregation. *Dev. Cell.* 2006; 10:575–585. [PubMed: 16580887]
19. Tang Z, Sun Y, Harley SE, Zou H, Yu H. Human Bub1 protects centromeric sister-chromatid cohesion through Shugoshin during mitosis. *Proc. Natl. Acad. Sci. U. S. A.* 2004; 101:18012–18017. [PubMed: 15604152]
20. Kitajima TS, Hauf S, Ohsugi M, Yamamoto T, Watanabe Y. Human Bub1 defines the persistent cohesion site along the mitotic chromosome by affecting Shugoshin localization. *Curr. Biol.* 2005; 15:353–359. [PubMed: 15723797]
21. Kitajima TS, et al. Shugoshin collaborates with protein phosphatase 2A to protect cohesin. *Nature.* 2006; 441:46–52. [PubMed: 16541025]
22. Gandhi R, Gillespie PJ, Hirano T. Human Wapl is a cohesin-binding protein that promotes sister-chromatid resolution in mitotic prophase. *Curr. Biol.* 2006; 16:2406–2417. [PubMed: 17112726]
23. Karamysheva Z, Diaz-Martinez LA, Crow SE, Li B, Yu H. Multiple anaphase-promoting complex/cyclosome degrons mediate the degradation of human Sgo1. *J. Biol. Chem.* 2009; 284:1772–1780. [PubMed: 19015261]
24. Xu Z, et al. Structure and function of the PP2A-shugoshin interaction. *Mol. Cell.* 2009; 35:426–441. [PubMed: 19716788]

25. Tanno Y, et al. Phosphorylation of mammalian Sgo2 by Aurora B recruits PP2A and MCAK to centromeres. *Genes Dev.* 2010; 24:2169–2179. [PubMed: 20889715]
26. McGuinness BE, Hirota T, Kudo NR, Peters JM, Nasmyth K. Shugoshin prevents dissociation of cohesin from centromeres during mitosis in vertebrate cells. *PLoS Biol.* 2005; 3:e86. [PubMed: 15737064]
27. Riedel CG, et al. Protein phosphatase 2A protects centromeric sister chromatid cohesion during meiosis I. *Nature.* 2006; 441:53–61. [PubMed: 16541024]
28. Domingo-Sananes MR, Kapuy O, Hunt T, Novak B. Switches and latches: a biochemical tug-of-war between the kinases and phosphatases that control mitosis. *Philos. Trans. R. Soc. B.* 2011; 366:3584–3594.
29. Solomon DA, et al. Mutational inactivation of STAG2 causes aneuploidy in human cancer. *Science.* 2011; 333:1039–1043. [PubMed: 21852505]
30. Orth M, et al. Shugoshin is a Mad1/Cdc20-like interactor of Mad2. *EMBO J.* 2011; 30:2868–2880. [PubMed: 21666598]
31. Llano E, et al. Shugoshin-2 is essential for the completion of meiosis but not for mitotic cell division in mice. *Genes Dev.* 2008; 22:2400–2413. [PubMed: 18765791]
32. Kawashima SA, Yamagishi Y, Honda T, Ishiguro K, Watanabe Y. Phosphorylation of H2A by Bub1 prevents chromosomal instability through localizing shugoshin. *Science.* 2010; 327:172–177. [PubMed: 19965387]
33. Yamagishi Y, Honda T, Tanno Y, Watanabe Y. Two histone marks establish the inner centromere and chromosome bi-orientation. *Science.* 2010; 330:239–243. [PubMed: 20929775]
34. Wu FM, Nguyen JV, Rankin S. A conserved motif at the C terminus of sororin is required for sister chromatid cohesion. *J. Biol. Chem.* 2011; 286:3579–3586. [PubMed: 21115494]
35. Wu N, et al. Scc1 sumoylation by Mms21 promotes sister chromatid recombination through counteracting Wapl. *Genes Dev.* 2012; 26:1473–1485. [PubMed: 22751501]

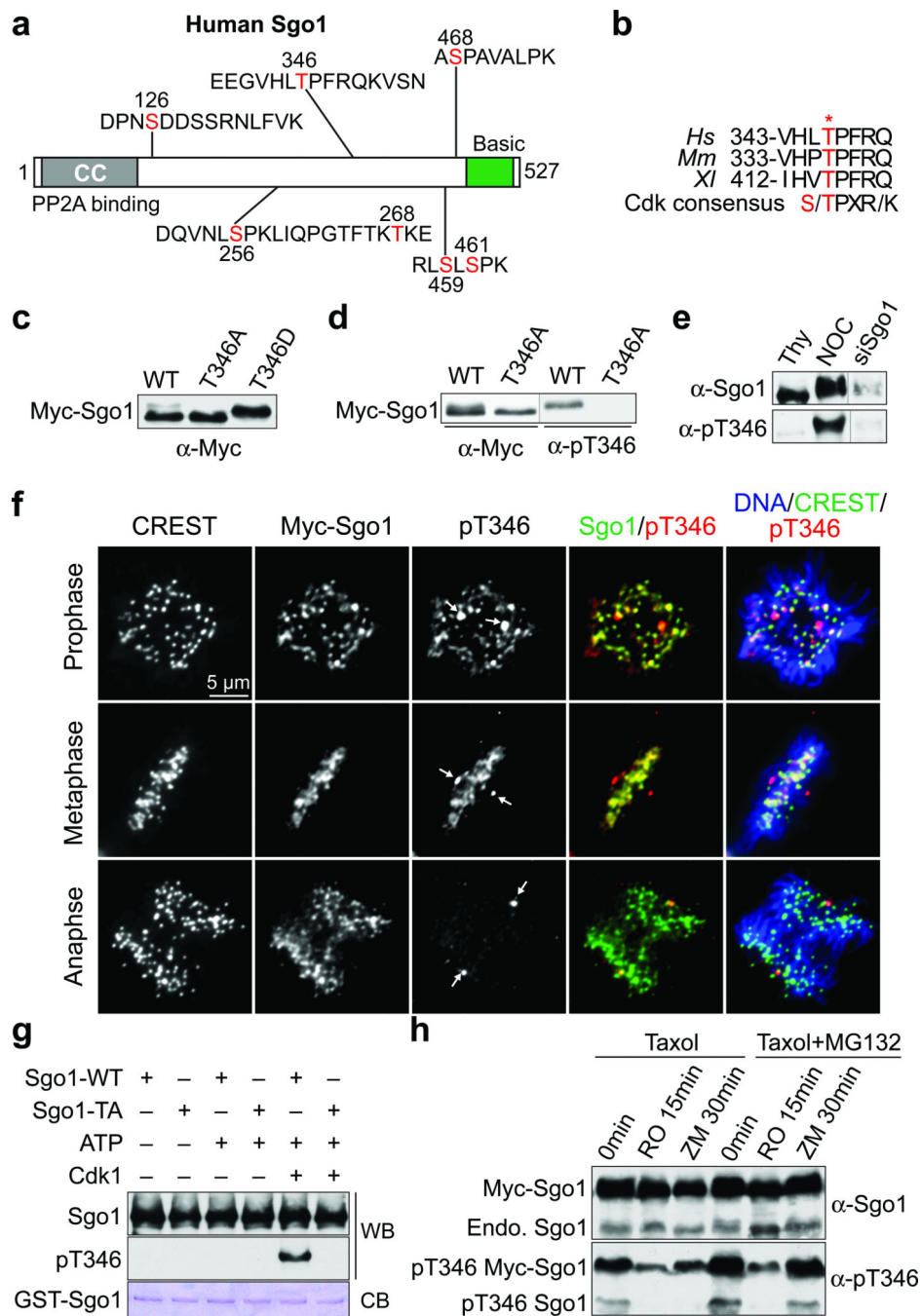


Figure 1. Human Sgo1 undergoes Cdk-dependent phosphorylation at T346 during mitosis
 (a) Schematic drawing of human Sgo1 showing its domain structures and the phosphopeptides and phosphorylation sites in mitosis identified with mass spectrometry in this study.
 (b) Alignment of sequences flanking the T346 site in Sgo1 proteins from human (Hs), mouse (Mm), and *Xenopus* (XI).
 (c) Lysates of HeLa Tet-On cells transfected with plasmids encoding Myc-Sgo1 WT, T346A, or T346D were blotted with α -Myc. (d) Lysates of HeLa Tet-On cells transfected with plasmids encoding Myc-Sgo1 WT or T346A were blotted with α -Myc (left panel) or α -pT346 Sgo1 (right panel). (e) α -Sgo1 IP of HeLa Tet-On cells

arrested at G1/S by thymidine (Thy), at mitosis by nocodazole (Noc), or transfected with siSgo1 were blotted with α -Sgo1 and α -pT346 Sgo1. Lanes are spliced together from the same gel. **(f)** Representative HeLa Tet-On cells stably expressing Myc-Sgo1 at different mitotic stages were stained with DAPI and the indicated antibodies. The arrows in the pT346 channel indicate nonspecific staining of centrosomes. **(g)** Recombinant GST-Sgo1 WT and T346A were incubated in the absence or presence of recombinant cyclin B-Cdk1 with or without ATP. The samples were resolved on SDS-PAGE and blotted with the indicated antibodies. The bottom panel shows Coomassie-blue staining of GST-Sgo1 proteins. **(h)** HeLa Tet-On cells stably expressing Myc-Sgo1 were blocked in mitosis by Taxol and treated with the Cdk1 inhibitor RO3306 and the Aurora kinase inhibitor ZM447439 without or without MG132 for the indicated times. Lysates of these cells were blotted with α -Sgo1 and α -pT346 Sgo1.

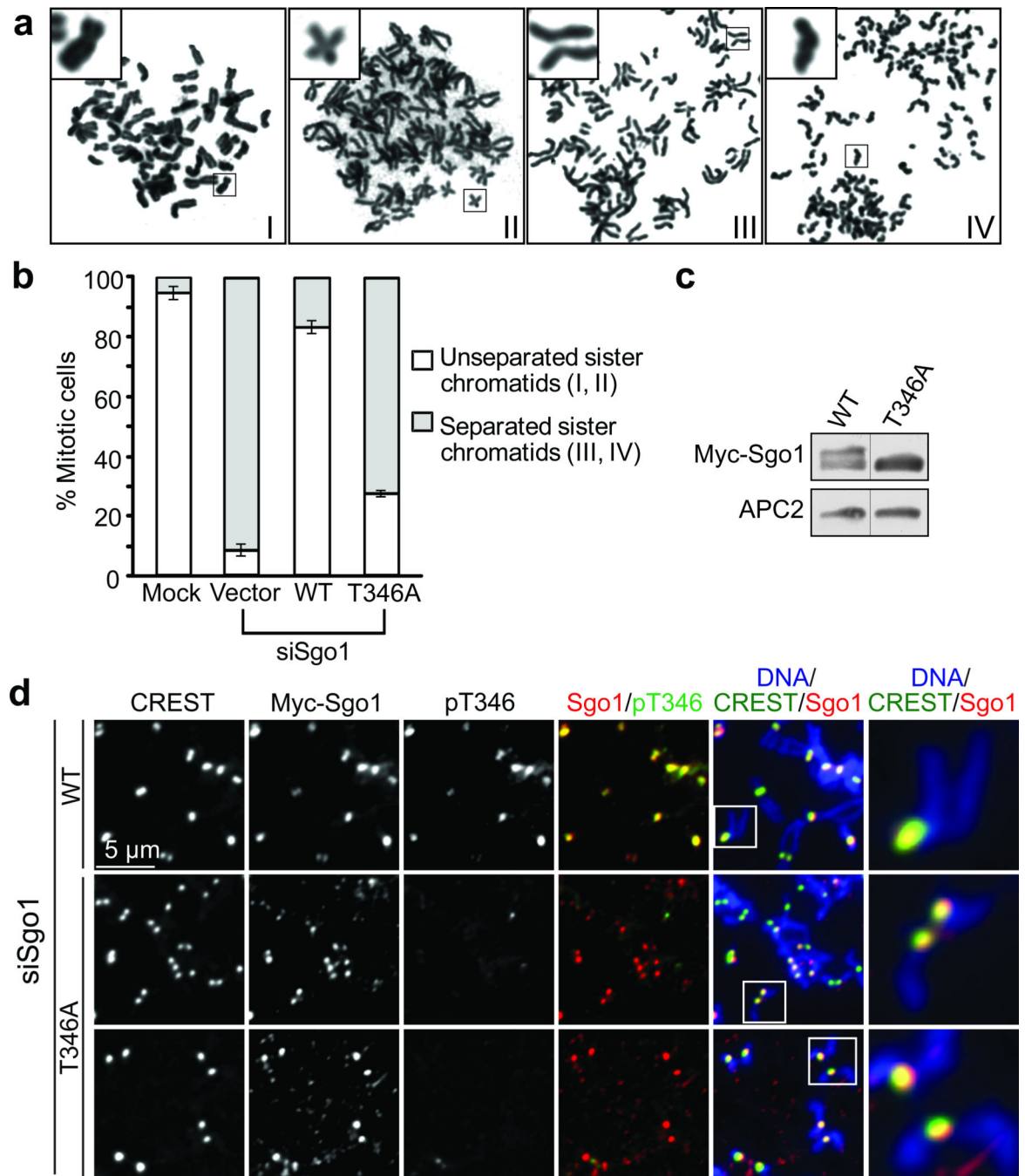


Figure 2. Sgo1 T346A localizes to centromeres, but is defective in sister-chromatid cohesion
(a) HeLa Tet-On cells transfected with vector or stably expressing RNAi-resistant Myc-Sgo1 WT or T346A were depleted of Sgo1 by RNAi, treated with nocodazole for 3 hr, and subjected to chromosome spreads. Four major chromosome morphology categories observed in chromosome spreads are shown. In category I, most chromosomes maintained cohesion at both centromeres and arms. In category II, most chromosomes maintained cohesion at centromeres, but lost arm cohesion. In category III, most sister chromatids were separated, but their pairing was maintained. In category IV, sister chromatids were separated,

hypercondensed, and scattered. Representative sister chromatids are magnified and shown in insets. **(b)** Quantification of the percentage of mitotic HeLa cells in **a** that contained unseparated (categories I and II) or separated (categories III and IV) sister chromatids. The mean and standard deviation of three independent experiments are shown. **(c)** Lysates of HeLa Tet-On cell stably expressing Myc-Sgo1 WT or T346A were blotted with α -Myc or α -APC2 (loading control). Lanes are spliced together from the same gel. **(d)** Mitotic HeLa Tet-On cells stably expressing Myc-Sgo1 WT or T346A were transfected with siSgo1 and stained with DAPI and the indicated antibodies. The boxed regions in the overlay were magnified and shown in the right panel.

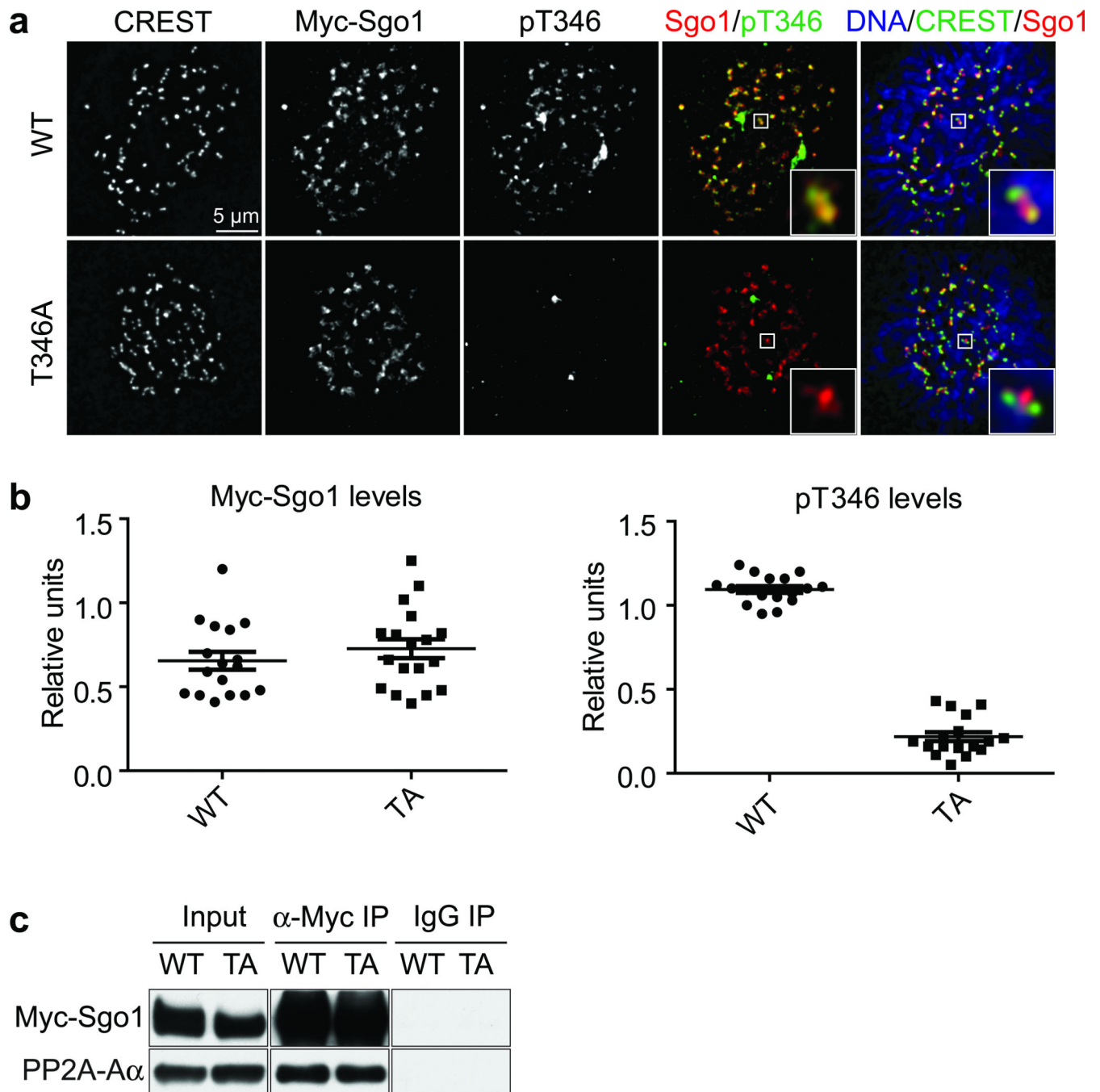


Figure 3. Sgo1 T346A localizes to centromeres and binds to PP2A

(a) Mitotic HeLa Tet-On cells stably expressing Myc-Sgo1 WT or T346A were stained with the indicated antibodies. The boxed areas in the overlay were magnified and shown in inset.

(b) Quantification of the intensities of α -Myc and α -pT346 Sgo1 staining of cells in a. Each dot in the graph represents a single cell (WT, n=18; T346, n=19).

(c) Lysates of mitotic cells in a were immunoprecipitated with IgG or α -Myc. The total cell lysate (Input), IgG IP, and α -Myc IP were blotted with the indicated antibodies.

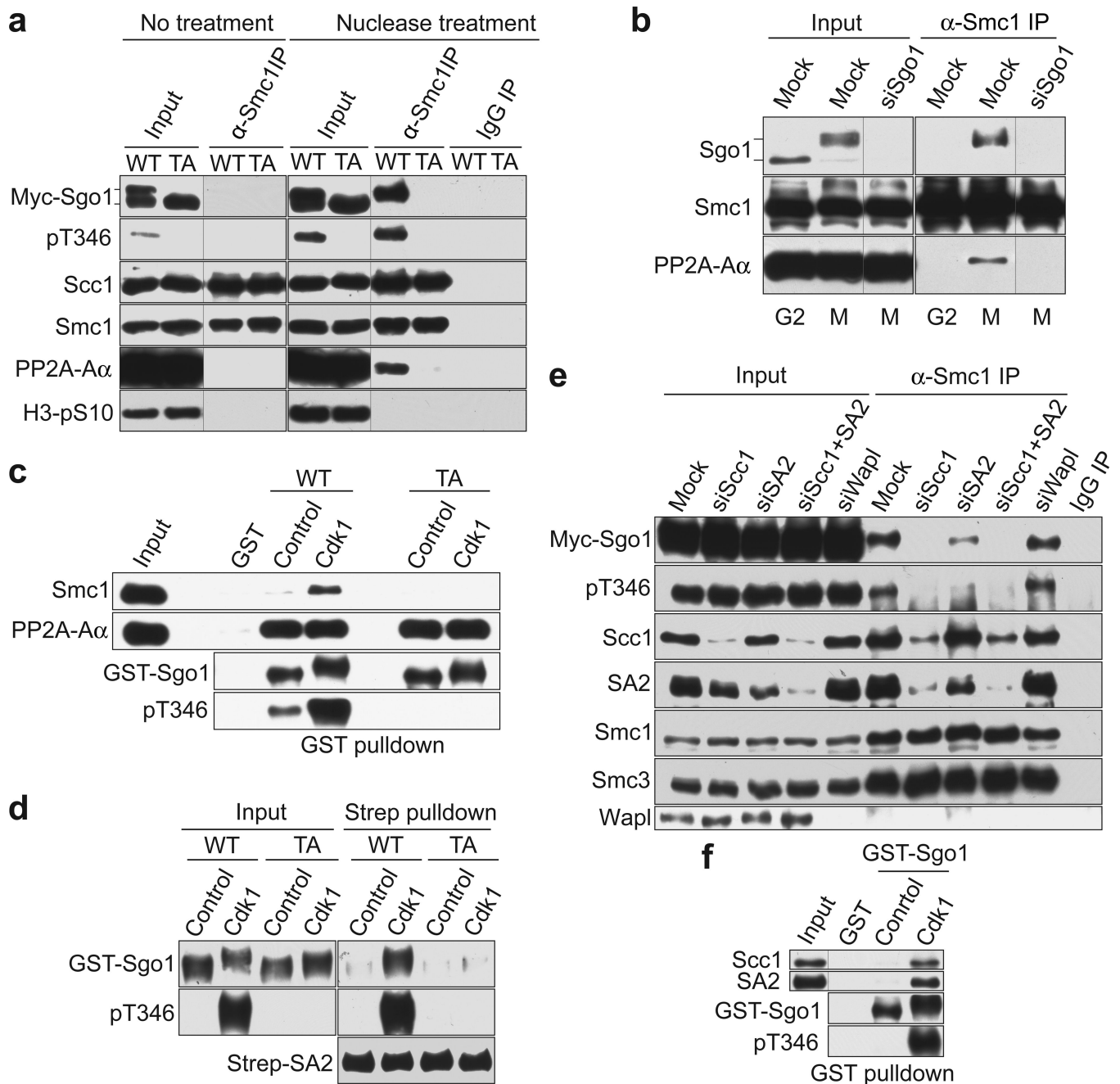


Figure 4. Sgo1 T346 phosphorylation promotes its binding to cohesin

(a) Mitotic HeLa Tet-On cells stably expressing Myc-Sgo1 WT or T346A (TA) were lysed with or without Turbo Nuclease. The total cell lysates (Input) and IgG/α-Smc1 immunoprecipitates (IP) were blotted with the indicated antibodies. (b) HeLa Tet-On cells were either mock transfected or transfected with siSgo1, collected at 7 hr after a thymidine block (G2) or in mitosis (M), and lysed with the nuclease-containing buffer. The total cell lysates and α-Smc1 IP were blotted with the indicated antibodies. (c) Glutathione-Sepharose beads bound to GST, GST-Sgo1 WT, or T346A (TA) proteins treated with buffer or cyclin B-Cdk1 were incubated with mitotic HeLa Tet-On cell extracts. The proteins bound to

beads were blotted with the indicated antibodies. **(d)** Lysates of mitotic HeLa Tet-On cells stably expressing StrepII-SA2 were incubated with Strep-Tactin beads. After washing, the beads were incubated with GST-Sgo1 WT or T346A (TA) that had been treated with buffer or cyclin B–Cdk1. The input Sgo1 proteins and proteins bound to beads were blotted with the indicated antibodies. **(e)** HeLa Tet-On cells stably expressing Myc-Sgo1 were mocked transfected or transfected with the indicated siRNAs, collected at mitosis, and lysed in the presence of nuclease. The total cell lysates (Input) and α -Smc1 IP were blotted with the indicated antibodies. IgG IP from mock transfected cells was used as a negative control. Note that the commercial Wapl antibody (Bethyl) failed to detect Wapl in α -Smc1 IPs. **(f)** GST or GST-Sgo1 pre-treated with buffer or cyclin B–Cdk1 were immobilized on glutathione-Sepharose beads. The beads were then incubated with lysates of Sf9 cells expressing recombinant human Scc1-His₆ and SA2. The Sf9 lysate (Input) and proteins bound to beads were blotted with the indicated antibodies.

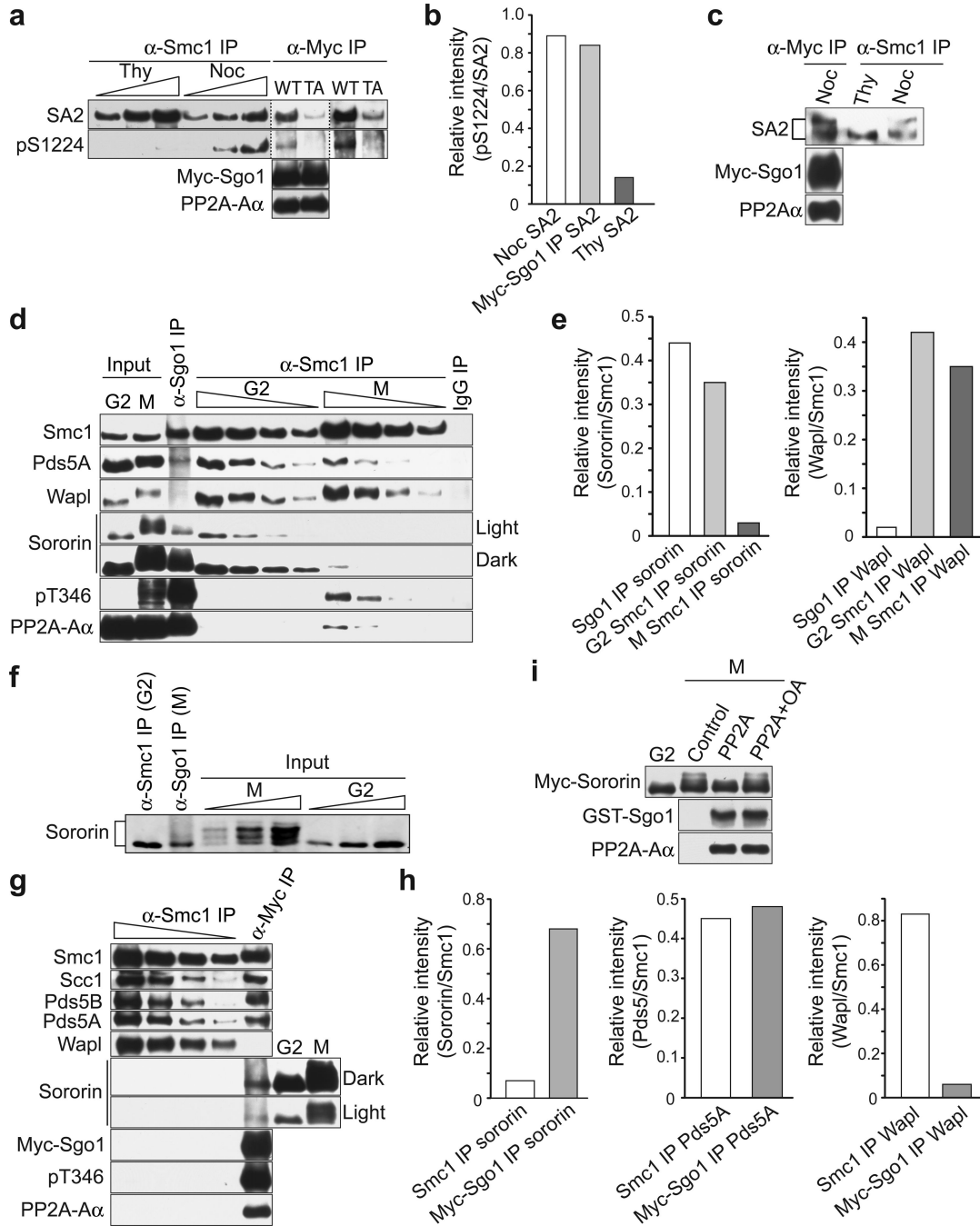


Figure 5. Sgo1-PP2A maintains cohesin-bound sororin in a hypophosphorylated state to counteract Wapl

(a) HeLa Tet-On cells stably expressing Myc-Sgo1 WT or T346A (TA) were arrested at G1/S with thymidine (Thy) or in mitosis by nocodazole (Noc). The α -Myc IP from the mitotic cell lysates and varying amounts of α -Smc1 IP from both lysates were blotted with α -SA2 or α -pS1224 SA2. For better comparison of the band intensities, a darker exposure of the α -SA2 or α -pS1224 SA2 blots of α -Myc IP is shown on the right. The α -Myc IP was also blotted with α -Myc and α -PP2A A α . (b) Quantification of the intensities of pS1224

SA2 in the IPs in **a** normalized by the intensities of total SA2 in the same IPs. The mean of two independent experiments is shown. **(c)** HeLa Tet-On cells stably expressing Myc-Sgo1 WT were arrested at G1/S with thymidine (Thy) or in mitosis by nocodazole (Noc). The α -Myc IP from the mitotic cell lysates and α -Smc1 IP from both lysates were blotted with α -SA2. To better reveal the SA2 gel mobility shift, we ran the gel for longer duration and with high concentrations of Mg^{2+} as reported previously¹⁵. **(d)** Sgo1-PP2A-bound cohesin contained Pds5 and hypophosphorylated sororin, but lacked Wapl. Lysates of HeLa Tet-On cells synchronized at G2 or mitosis (M) were immunoprecipitated with α -Sgo1 or α -Smc1. The total lysates (Input), α -Sgo1/IgG IPs from the mitotic lysate, and varying amounts of α -Smc1 IPs from both lysates were blotted with the indicated antibodies. Note that Wapl was readily detected in α -Smc1 IPs when blotted with our own α -Wapl antibody. **(e)** Quantification of the intensities of sororin and Wapl in the IPs in **c** normalized by the intensities of Smc1 in the same IPs. The mean of two independent experiments is shown. **(f)** Lysates of HeLa Tet-On cells synchronized at G2 or mitosis (M) were immunoprecipitated with α -Sgo1 or α -Smc1. The total lysates in varying amounts (Input), α -Sgo1 IP from the mitotic lysate, and α -Smc1 IP from G2 lysate were blotted with anti-sororin. **(g)** Lysates of mitotic HeLa Tet-On cells stably expressing Myc-Sgo1 were immunoprecipitated with α -Smc1 or α -Myc. The α -Myc IP and varying amounts of α -Smc1 IP were blotted with the indicated antibodies. The lysates of the same cells synchronized in G2 or mitosis (M) were blotted with α -sororin to indicate the positions of the hypo- or hyper-phosphorylated sororin species. **(h)** Quantification of the intensities of sororin, Pds5A, and Wapl in the IPs in **g** normalized by the intensities of Smc1 in the same IPs. The mean of two independent experiments is shown. **(i)** HeLa Tet-On cells stably expressing Myc-Sgo1 were cultured in the presence of doxycycline, mock transfected or transfected with siSororin, and synchronized in mitosis. The total cell lysates (Input) and the α -Myc IP were blotted with the indicated antibodies.

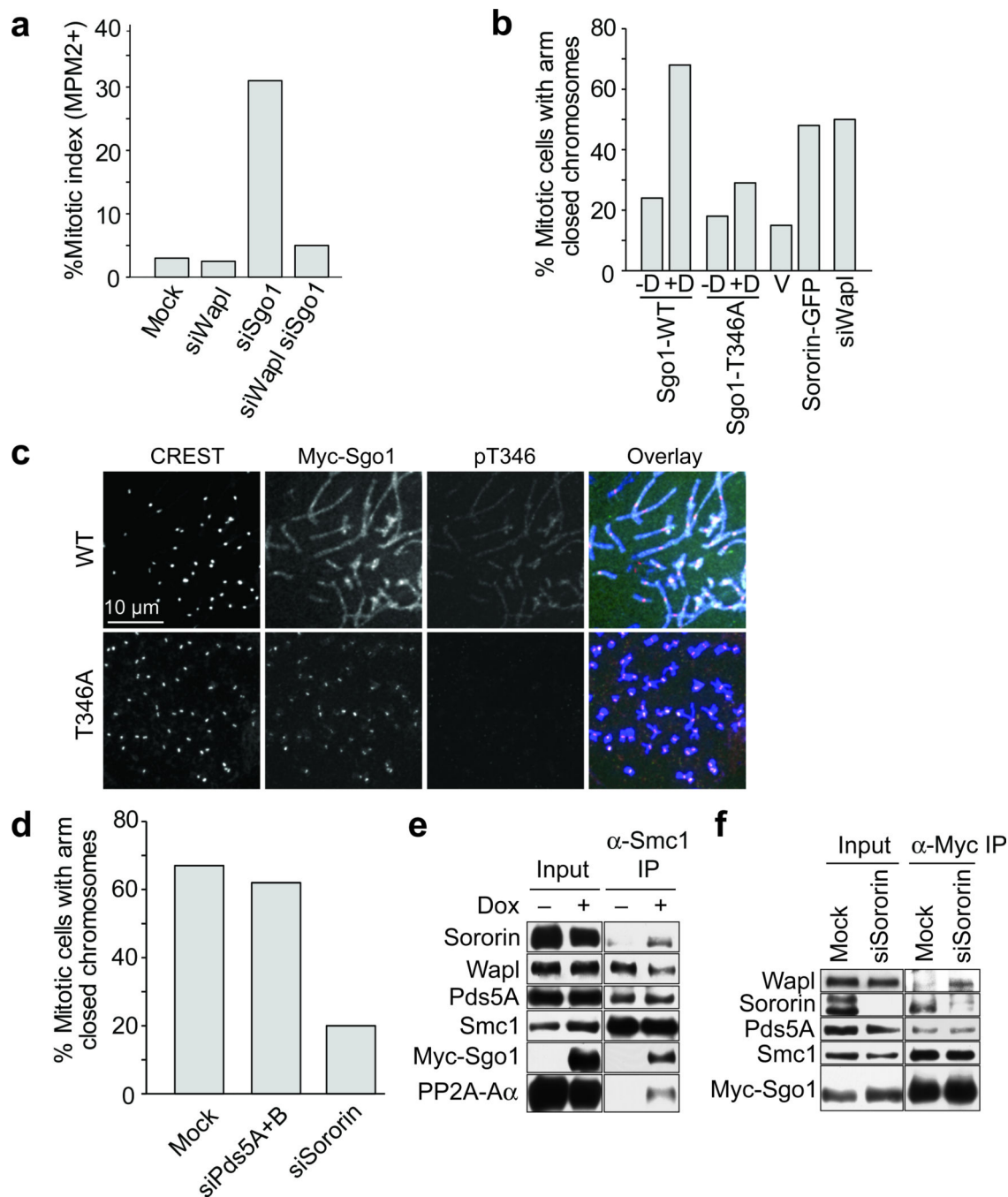


Figure 6. Sororin is required for the ectopic arm cohesion induced by Sgo1 overexpression
(a) Co-depletion of Wapl rescued the mitotic arrest caused by Sgo1 depletion. HeLa Tet-On cells were transfected with the indicated siRNAs for 24 hr and analyzed by FACS. The mitotic index (as determined by the percentage of MPM2-positive cells) was plotted. The mean of two independent experiments is shown. **(b)** Overexpression of Sgo1 or sororin caused ectopic cohesion on chromosome arms. HeLa Tet-On cells stably expressing Myc-Sgo1 WT, T346A, or sororin-GFP or HeLa Tet-On cells transfected with siWapl were treated with nocodazole for 3 hr. The Myc-Sgo1-expressing cells were cultured in the

absence (–) or presence (+) of doxycycline (Dox). Mitotic cells were collected and subjected to chromosome spread. The percentage of mitotic cells with closed chromosome arms (category I in Fig. 2a) was scored and plotted. The mean of two independent experiments is shown. (c) Mitotic cells expressing Myc-Sgo1 WT or T346A in the presence of Dox described in **b** were stained with the indicated antibodies. (d) HeLa Tet-On cells stably expressing Myc-Sgo1 WT were cultured in the presence of Dox and transfected with the indicated siRNAs. After treatment with nocodazole for 3 hr, the mitotic cells were subjected to chromosome spread and stained with DAPI. The percentage of mitotic cells with closed chromosome arms (category I in Fig. 2a) was scored and plotted. The mean of two independent experiments is shown. (e) Lysates of mitotic (M) HeLa Tet-On cells transiently expressing Myc-sororin were immunoprecipitated with α -Myc. The α -Myc beads were incubated with the partially purified GST-Sgo1–PP2A complex in the presence or absence of okadaic acid (OA). The reaction mixtures were blotted with the indicated antibodies. (f) HeLa Tet-On cells stably expressing Myc-Sgo1 were cultured in the absence (–) or presence (+) of doxycycline (Dox) and synchronized in mitosis. The total cell lysates (Input) and the α -Smc1 IP were blotted with the indicated antibodies.

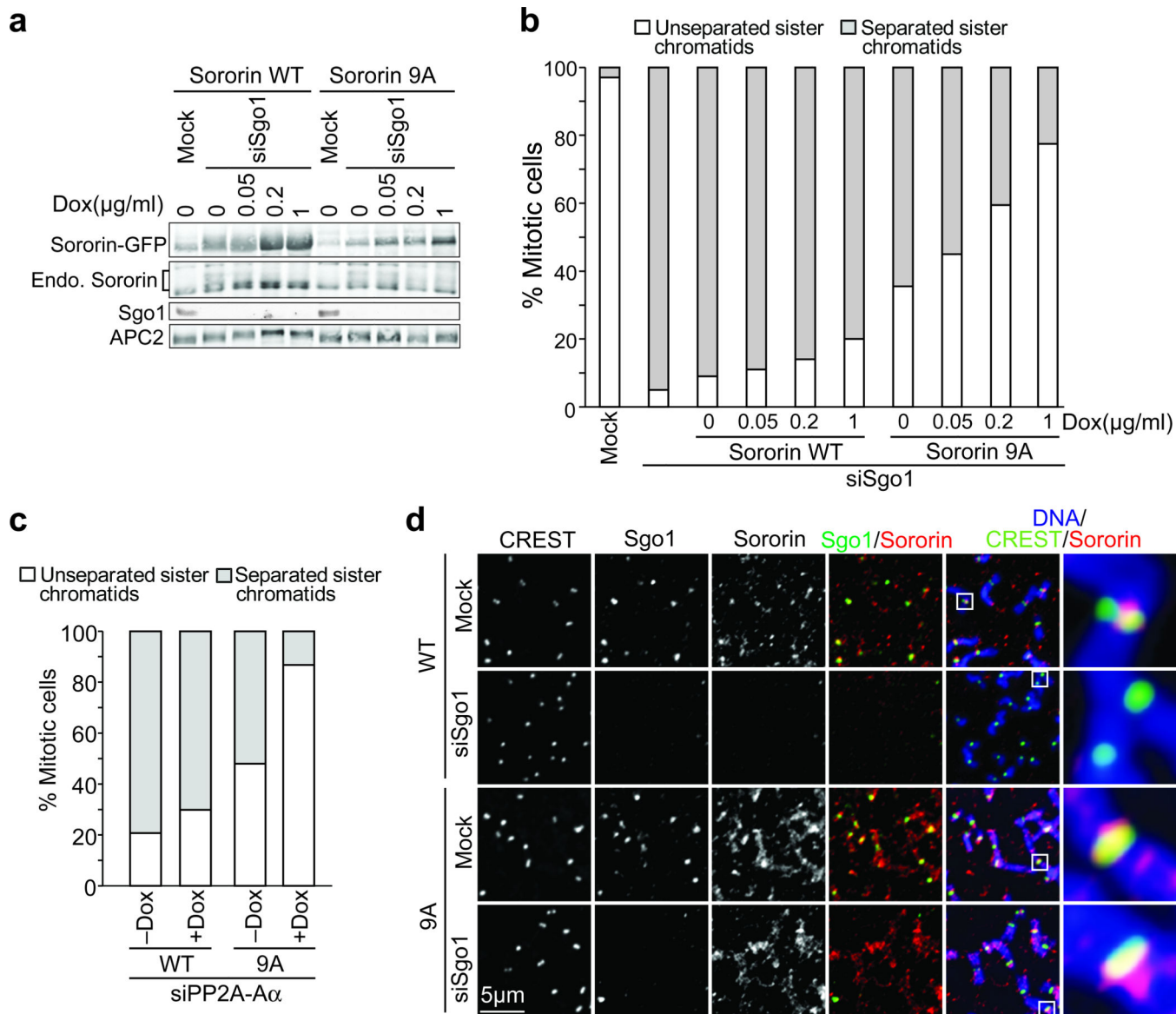


Figure 7. Expression of non-phosphorylatable sororin bypasses the requirement for Sgo1–PP2A in cohesion

(a) HeLa Tet-On cells stably expressing sororin-GFP WT or 9A were cultured in the absence or presence of varying concentrations of doxycycline (Dox) and mock transfected or transfected with siSgo1. Cell lysates were blotted with anti-sororin (which detected both sororin-GFP and the endogenous sororin), anti-Sgo1, and anti-APC2 antibodies. (b) Mitotic cells in a were subjected to chromosome spreads. The percentages of mitotic cells with separated or unseparated chromatids were quantified. The mean of two independent experiments is shown. (c) HeLa Tet-On cells stably expressing sororin-GFP WT or 9A were cultured in the absence (–) or presence (+) of doxycycline (Dox) and transfected with siPP2A A α . Mitotic cells were collected and subjected to chromosome spreads. The percentages of mitotic cells with separated or unseparated chromatids were quantified. The mean of two independent experiments is shown. (d) Mitotic cells in a (1 μ g/ml Dox) were

stained with the indicated antibodies. The boxed regions in the overlay were enlarged and shown on the right.

Author Manuscript

Author Manuscript

Author Manuscript

Author Manuscript

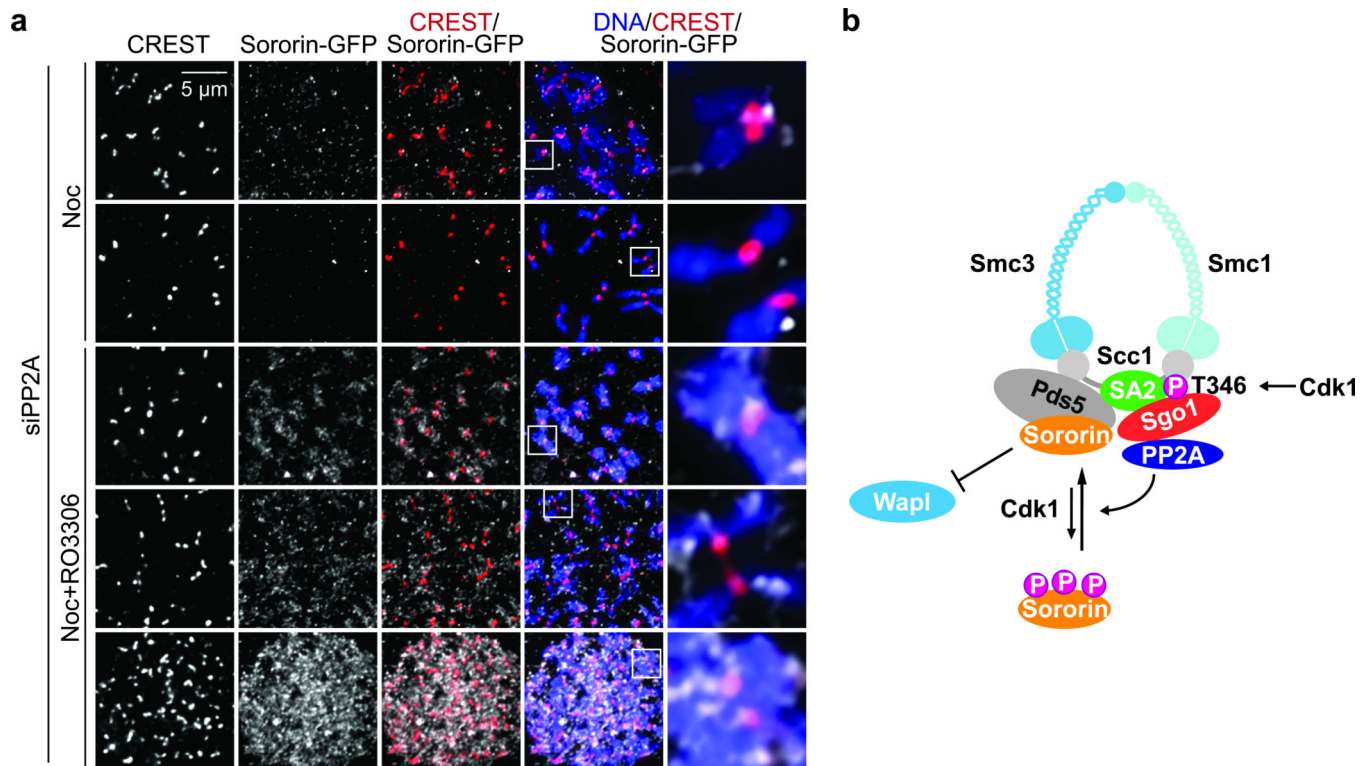


Figure 8. Sororin dissociation from mitotic chromosomes requires Cdk1

(a) HeLa Tet-On cells stably expressing sororin-GFP transfected with siPP2A Aa were synchronized by a thymidine-arrest-release protocol. At 8 hrs after thymidine release, nocodazole was added to arrest cells in mitotic for 3 hrs. Mitotic cells were collected and were either untreated or treated with the Cdk1 inhibitor RO3306 (10 μ M) for 15 min. The cells were stained with DAPI and the indicated antibodies. The boxed regions in the overlay were enlarged and shown on the right. (b) Model for how Sgo1–PP2A maintains centromeric cohesion during mitosis in human cells.